Interrogating DNA methylation associated with Lewy body pathology in a cross brain-region and multi-cohort study.

Joshua Harvey[1+], Jennifer Imm[1+], Morteza Kouhsar[1], Adam R. Smith[1], Byron Creese[1,2], Rebecca G. Smith[1], Gregory Wheildon[1], Leonidas Chouliaras[3,4], Gemma Shireby[5], Zane Jaunmuktane[6], Eduardo De Pablo-Fernández[6], Thomas Warner[6], Debbie Lett[7], Djordje Gveric[8], Hannah Brooks[9], Johannes Attems[7], Alan Thomas[7], Emma Dempster[1], Clive Ballard[1], John T O'Brien[3], Dag Aarsland[10], Jonathan Mill[1], Lasse Pihlstrøm[11], Ehsan Pishva[1,12,†], Katie Lunnon[1,†,*]

1 Department of Clinical and Biomedical Science, Faculty of Health and Life Sciences, University of Exeter, Exeter, UK

2 Department of Life Sciences, College of Health, Medicine and Life Sciences, Brunel University of London, London, UK

3 Department of Psychiatry, University of Cambridge School of Clinical Medicine, Cambridge, UK

4 Specialty Dementia and Frailty Service, Essex Partnership University NHS Foundation Trust, St Margaret's Hospital. Epping, UK

5 Great Ormond Street Hospital, University College London, London, UK

6 Queen Square Brain Bank for Neurological Disorders, University College London Queen Square Institute of Neurology, University College London, London, UK

7 Newcastle Brain Tissue Resource, Newcastle University, Newcastle, UK

8 MS and Parkinson's Tissue Bank, Department of Brain Sciences, Imperial College London, London, UK

9 The Oxford Brain Bank, University of Oxford, Oxford, UK

10 Institute of Psychiatry, Psychology & Neuroscience (IoPPN), Kings College London, UK

11 Institute of Clinical Medicine, Oslo University Hospital, Oslo, Norway.

12 Department of Psychiatry and Neuropsychology, School for Mental Health and Neuroscience (MHeNS), Maastricht University, Maastricht, The Netherlands

+These authors contributed to this study equally

† These authors contributed to this study equally

* Corresponding author: Katie Lunnon, RILD, Barrack Road, University of Exeter, Devon, UK. UK. Email address: k.lunnon@exeter.ac.uk

ABSTRACT

Lewy body (LB) diseases are an umbrella term encompassing a range of neurodegenerative conditions all characterized by the hallmark of intra-neuronal α-synuclein associated with the development of motor and cognitive dysfunction. In this study, we have conducted a large meta-analysis of DNA methylation across multiple cortical brain regions, in relation to increasing burden of LB pathology. Utilizing a combined dataset of 1239 samples across 855 unique donors, we identified a set of 30 false discovery rate (FDR) significant loci that are differentially methylated in association with LB pathology, the most significant of which were located in *UBASH3B* and *PTAFR*, as well as an intergenic locus. Ontological enrichment analysis of our meta-analysis results highlights several neurologically relevant traits, including synaptic, inflammatory and vascular alterations. We leverage our summary statistics to compare DNA methylation signatures between different neurodegenerative pathologies and highlight a shared epigenetic profile across LB diseases, Alzheimer's disease and Huntington's disease, although the top-ranked loci show disease specificity. Finally, utilizing summary statistics from previous large-scale genome-wide association studies we report FDR significant enrichment of DNA methylation differences with respect to increasing LB pathology in the *SNCA* genomic region, a gene previously associated with Parkinson's disease and dementia with Lewy bodies.

KEYWORDS

Alpha-synuclein (α-synuclein), Brain, Dementia, DNA methylation, Epigenome-wide-association study (EWAS), Lewy body (LB), Meta-analysis, Parkinson's disease (PD), Dementia with Lewy bodies (DLB), SNCA

INTRODUCTION

The Lewy body diseases (LBDs) including Parkinson's disease (PD), Parkinson's disease dementia (PDD) and Dementia with Lewy bodies (DLB), are neurodegenerative diseases classified by the accumulation of alpha-synuclein (α-synuclein) in neurons, forming Lewy bodies (LBs). Collectively these diseases are the second most common cause of neurodegeneration and dementia, following Alzheimer's disease (AD) and confer a high care giver burden, given the complex nature of the disease and symptoms (Ricci et al., 2009; Lee et al., 2013; Svendsboe et al., 2016). According to diagnostic criteria, DLB and PDD are distinguished clinically based on the timing of onset of parkinsonism and dementia symptoms (McKeith et al., 2017). At post-mortem examination these disorders present similar underlying pathological profiles, with in addition to LBs, mixed pathology of neurofibrillary tangles (NFT) and amyloid beta (Aβ) plaques commonly featuring.

Over the last few years more studies have been undertaken to investigate the genetic mechanisms underpinning PD (Kim et al., 2024) and DLB (Chia et al., 2021). These studies have highlighted numerous risk loci associated with these diseases, including 78 loci in PD (Kim et al., 2024) and five genome wide significant loci in DLB, three being known PD risk genes (*SNCA*, *GBA* and *TMEM175*) and two being AD risk genes (*APOE* and *BIN1*) (Chia et al., 2021). However, whilst these studies have provided novel insight into disease pathways, genetic variation only explains a small amount of disease susceptibility, with environmental factors also being robustly associated with disease development and progression (Tsalenchuk et al., 2023; Ben-Shlomo et al., 2024; An and Xu, 2024). In recent years there has been a growing appreciation that epigenetic mechanisms may mediate the interaction between genetic and environmental risk factors in the etiology of sporadic neurodegenerative diseases. Indeed, several epigenome-wide association studies (EWAS) have now been performed in AD, which have culminated in several large-scale meta-analyses, nominating numerous robust and reproducible alterations in DNA methylation in the cortex during disease (Lunnon et al., 2014; De Jager et al., 2014; Smith et al., 2019; Shireby et al., 2022; Smith et al., 2021). However, there has been considerably less research exploring DNA methylomic signatures in LB pathology spectrum disease, with in fact only one EWAS performed to date with a substantial sample size (n > 100) and utilizing multiple independent cohorts (Pihlstrøm et al.

2022). That study utilized the Illumina Infinium MethylationEPIC array to quantify DNA methylation in the prefrontal cortex (PFC) in a primary discovery analysis from 73 control and 249 LB disease spectrum patients from the Netherlands Brain Bank (NBB). Their analysis focussed on changes associated with LB pathology development, irrespective of the primary diagnosis and reported 24 loci significantly associated with Braak LB stage, with a strong concordance of the direction of effect with findings from the independent Brains for Dementia Research (BDR) cohort. Among the reported loci, four CpG sites were significant in both cohorts, annotated to *TMCC2*, *SFMBT2*, *AKAP6*, and *PHYHIP*.

To investigate the epigenetic underpinnings of these diseases in relation to neuropathology, we have designed the largest EWAS of LBDs to date, which includes multiple cortical brain regions and a meta-analysis with three independent cohorts. Our analyses utilized 1239 samples from 855 unique donors and identified 30 false discovery rate (FDR) significant loci associated with LB pathology in the cortex. Leveraging prior studies of DNA methylation undertaken in AD and Huntington's Disease (HD), we found shared epigenomic profiles between neurodegenerative diseases and identified epigenomic signatures to distinguish different pathologies. Finally, we identified sites with evidence of genetic influence on DNA methylation levels and demonstrate an enrichment of methylation in the *SNCA* gene in LBDs.

RESULTS

Meta analysis of differential DNA methylation associated with cortical Lewy bodies

Utilizing a dataset comprising three independent cohorts with DNA methylation profiling conducted on the Illumina Infinium MethylationEPIC v1.0 array, we sought to test for associations with LB pathology, as measured by the Braak LB Staging criteria. The cohort included novel data generated from the UK Brain Bank Network (UKBBN, n = 801 samples, 417 individual donors, n = 398 Anterior Cingulate Cortex (ACC), n = 403 Prefrontal Cortex (PFC)) and data from two existing datasets: the Netherlands Brain Bank (NBB, n = 322 PFC donors) (Pihlstrøm et al., 2022) and Brains for Dementia Research (BDR, n = 116 PFC donors) (Shireby et al., 2022) (**Figure 1**). Separately for each cohort, we used linear regression to identify differentially methylated positions (DMPs) associated with LB pathology, including confounding variables (age, sex, cell type proportions, technical batch variables, post-mortem interval and Braak NFT stage) and surrogate variables as required to ensure that the genomic inflation lambda value < 1.2 (**Methods**), (**Supplementary Figure 1**). All donors in this dataset where either controls without neurodegenerative disease or required a primary neuropathologically confirmed diagnosis of incidental Lewy Body Disease (iLBD), PD, PDD or

DLB (**Methods**). Given that 50-80% of LBDs have concomitant AD pathology (Robinson et al., 2018), where possible we minimized the number of individuals with advanced Braak NFT stage in our cohorts based on inclusion criteria for a neuropathological primary diagnosis of LBD (**Figure 1**, **Supplementary Table 1, Methods**). We further included Braak NFT as a covariate in our primary discovery models (**Methods**). We conducted a fixed effect, inverse variance weighted meta-analysis of the three cohorts (total sample size = 1239, unique donors = 855) for 774,310 methylation sites passing data quality control (QC). We identified three differentially methylated positions (DMP's) associated with LB pathology stage at a genome-wide significance association threshold of $p < 9 \times 10^{-8}$ (**Figure 2A&B**), whilst a further 27 DMPs were identified at a more lenient false FDR corrected p-value threshold (q-value < 0.05) (**Figure 2A**, **Supplementary Table 2, Supplementary Figure 2**).

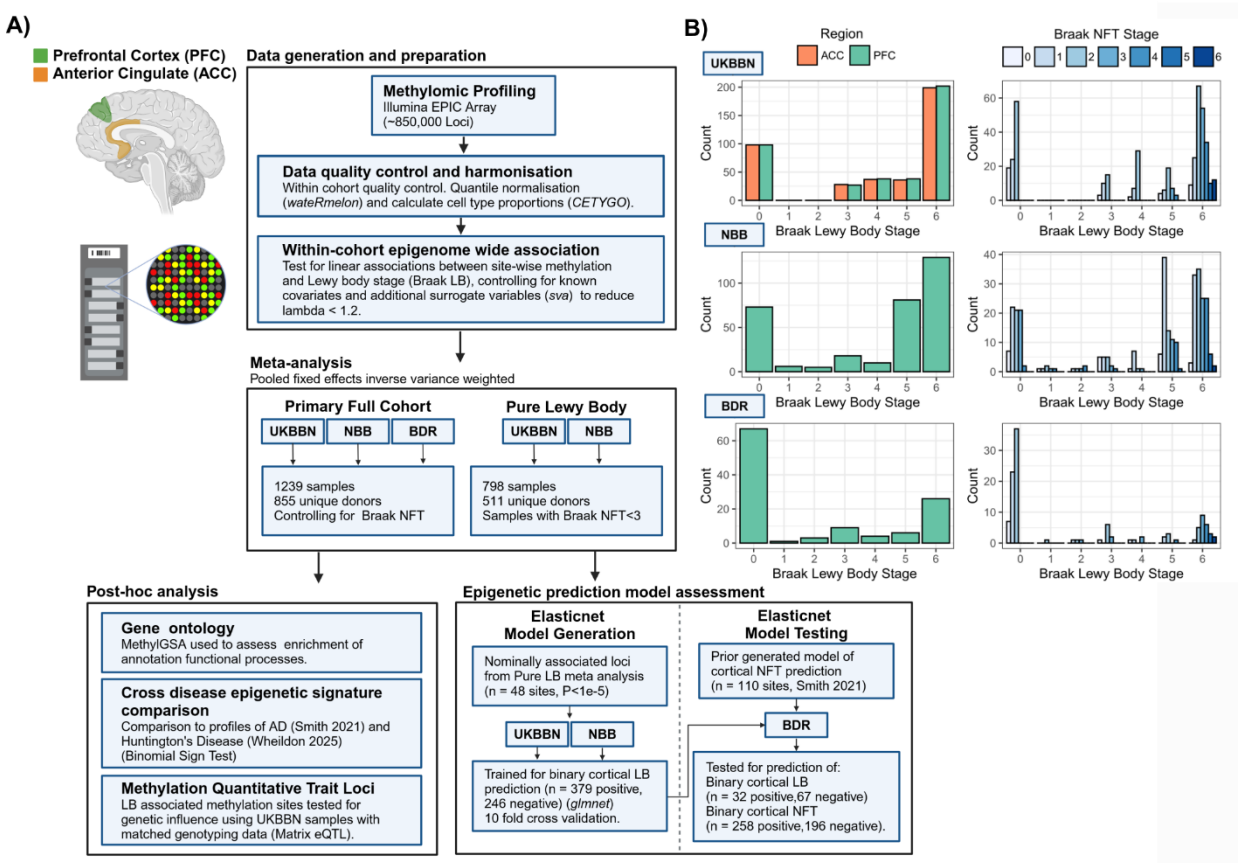

Figure 1. Cohort summary of samples used in DNA methylation association meta-analysis of Lewy bodies. A) Brain regions and analysis protocol for meta-analyses. Brain regions include two cortical regions, the prefrontal cortex (PFC, BA9) and the anterior cingulate cortex (ACC, BA24). Analysis plan outlining steps in data generation, harmonization, within cohort linear association analyses and fixed effects meta-analysis. **B)** Summary of sample numbers in the UK Brain Bank Network (UKBBN), Netherlands Brain Bank (NBB) and Brains for Dementia Research (BDR) cohorts. Left hand bar plots show number of samples per Braak LB Stage, right hand plots show number of samples with coinciding AD pathology as measured by the Braak NFT stage. Components of figure created in https://BioRender.com

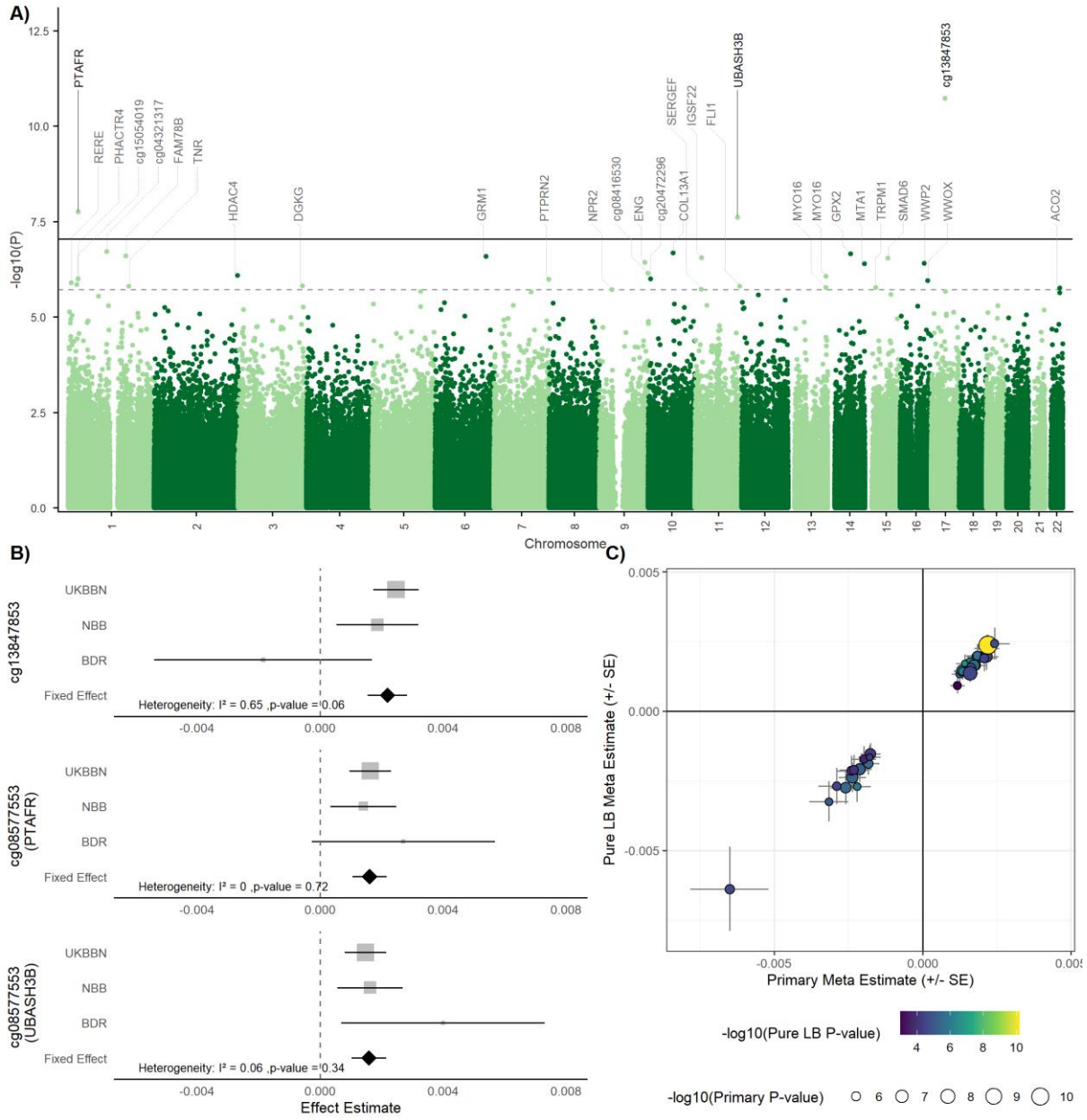

Figure 2. DNA methylation associated with Lewy body Braak stage in a cross cortical meta-analysis. A) Manhattan plot showing differentially methylated sites associated with Braak LB stage in a fixed effects inverse variance weighted meta-analysis of 1239 total samples (primary full cohort LB pathology meta-analysis). Y-axis shows -log10 transformed p-value of association, x-axis shows chromosomal positions (chromosomes 1-22). The black solid horizontal line shows the genome-wide significance threshold ($p < 9 \times 10^{-8}$), whilst the grey dashed horizontal line denotes the FDR-corrected significance threshold ($q < 0.05$). Points are colored to show chromosome number and for those that passed the significance thresholds annotated by UCSC gene symbols in the Illumina manifest file and where unavailable, Illumina CpG ID is displayed. **B)** Forest plots of the effect sizes for the three sites passing the genome-wide significance threshold in the primary full cohort LB pathology meta-analysis. Grey points show cohort specific estimates, sized by weight in the inverse variance weighted meta-analysis. Whiskers show 95% confidence interval (CI) of estimate. Diamonds show effect estimates and 95% CI for fixed effect estimates from the primary meta-analyses. The I^2 heterogeneity statistic and heterogeneity p-value are displayed for each site. **C)** Correlation plot of effect sizes between the primary full cohort LB pathology meta-analysis (y-axis) versus a subset analysis of samples without substantial coincident AD pathology (Braak NFT stage ≤ II) (x-axis) for the 30 FDR-significant DMPs identified in the primary full cohort meta-analysis. Points are sized by -log10 transformed p-value significance in the primary full meta-analysis and colored by -log10 transformed p-value significance in the pure LB subset analysis. Effect sizes are displayed as change in methylation (beta value) per increasing LB Braak stage.

Although we had controlled for Braak NFT stage in our primary meta-analysis, we wanted to further demonstrate that coinciding AD related NFT pathology was not driving our findings, through the exclusion of samples with a Braak NFT score of three or greater. This reduced our total sample size and number of viable cohorts, with only the UKBBN and NBB retaining enough samples to adequately conduct the within cohort EWAS prior to meta-analysis, giving us a total sample size of 798 for this "pure LB" secondary subset cohort analysis (representing 511 unique donors). As expected from this reduced sample size, we observed a reduced number of significant DMPs, with only one site passing both thresholds for significance (cg13847853) (**Supplementary Table 3**). However, despite this, we found that the effect size of the 30 FDR significant DMPs we had identified in the primary full cohort analysis were highly correlated with the effect size from this pure LB secondary subset cohort analysis (Pearson's correlation (r) = 0.997, $p = 1.26 \times 10^{-32}$), with a 100% concordance in the direction of effect (**Figure 2C**). Standard error estimates were also highly comparable between the two analyses (Pearson's r = 0.998, $p = 2.11 \times 10^{-35}$). Furthermore, although only one of the primary full cohort meta-analysis DMPs passed the genome-wide significance threshold in this secondary pure LB pathology subset cohort meta-analysis, 15 of the sites still passed the suggestive threshold for association ($p < 1 \times 10^{-5}$), with the largest p-value for any of the 30 sites still being nominally significant ($p < 1.04 \times 10^{-3}$). Together this indicates that the associations identified in the primary full cohort analysis are not dependent on the presence of concomitant NFT pathology, and that the loss of significance in this secondary subset analysis is principally a result of reduced power. The top result in both analyses, annotated to probe cg13847853, is a DMP with previous significant association to AD NFT pathology (Shireby et al., 2022; Smith et al., 2021) and is novel in the context of LB disease. It represents an intergenic locus located between the protein coding genes *KRT19* (-11,777 base-pairs) and *KRT9* (+31,973 base-pairs). It is also proximal to the long non-coding RNA gene *LINC00974* (+ 9,522 base-pairs).

Ontological enrichment analysis highlights neuronal processes and *SNCA* as a gene of interest

Next to determine potential biological function underpinning the methylation signature identified in our primary full cohort LB pathology meta-analysis, we employed gene ontology (GO) analysis on genes identified in the primary meta-analysis, identifying a set of nine FDR-significant enriched terms (**Figure 3A**, **Supplementary Table 4**). This included a number of terms relevant to neuronal and synaptic function (dendritic spine, positive regulation of neurogenesis, regulation of nervous system process and intrinsic component of post-synaptic membrane), inflammation (tertiary granule), vascular function (platelet activation) and broader cellular processes (e.g., regulation of lipase activity, positive regulation of histone

modification). The method employed for the ontological analyses, which aggregates methylation around gene annotations to provide a set of genes to be tested for over representation analysis using robust rank aggregation (RRA), identified 245 genes as significant based on the fixed-effect p-value from our primary full cohort LB pathology meta-analysis (**Supplementary Table 5**). Notably, this included the *SNCA* gene, which had not featured in the top results from our primary full cohort meta-analysis but is of considerable interest given it encodes for α-synuclein. Exploring this region in more detail, we saw that seven loci in the *SNCA* gene showed evidence of a nominal association (uncorrected $p < 0.05$), all residing in the 5' region of the gene and showing hypomethylation with increasing LB stage (**Supplementary Figure 3**).

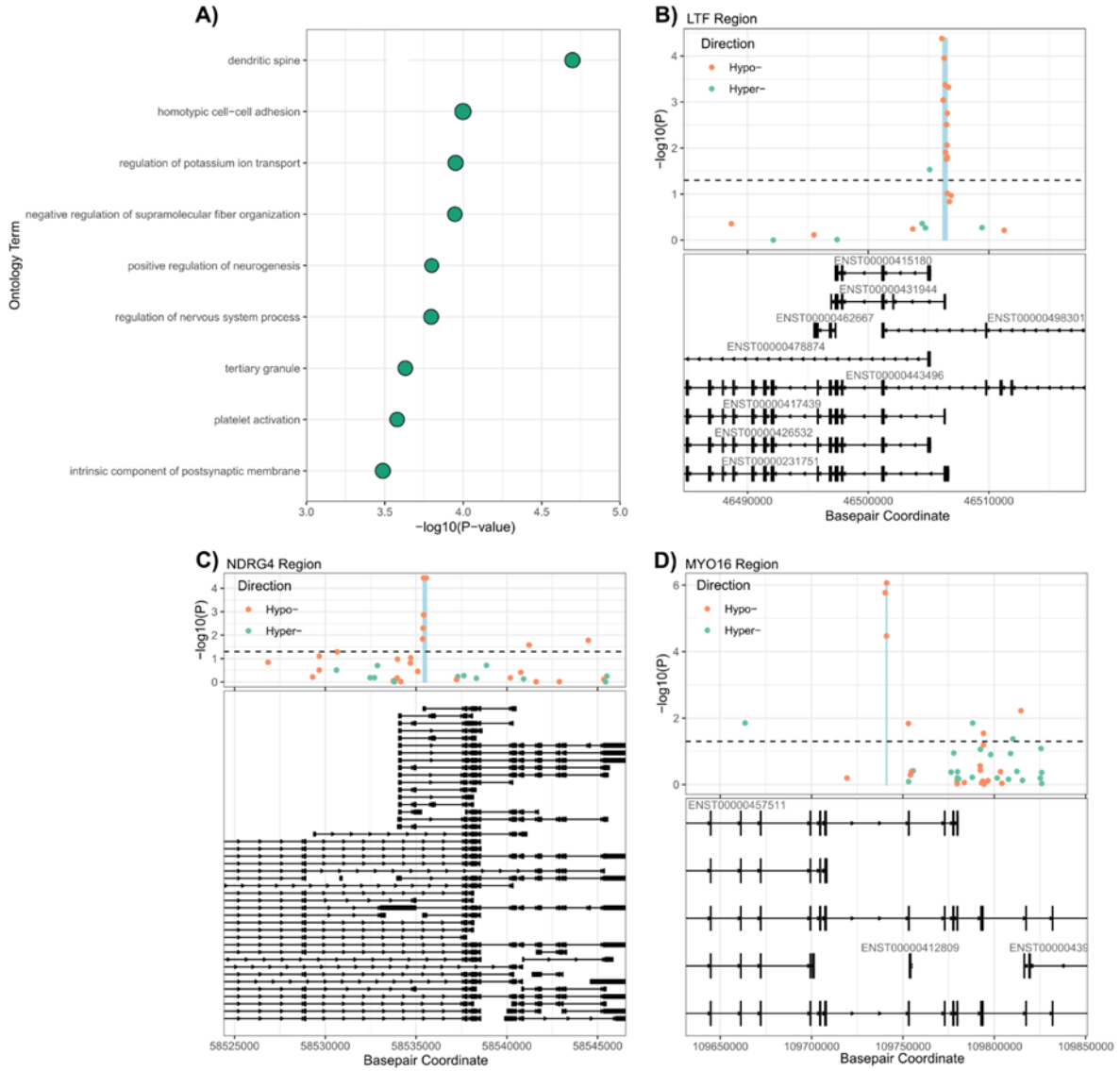

Figure 3. A) Gene ontology (GO) analysis of primary full cohort Lewy body pathology meta-analysis. The nine FDR-significant terms identified in the ontological analysis are shown, with -log10 transformed raw p-value shown on the x-axis. REVIGO prioritized gene parent terms are shown on the y-axis. **B)** Mini-Manhattan plots of the *LTF* gene region, **C)** *NDRG4* gene region and **D)** *MYO16* gene region. Y-axis shows -log10 transformed p-

value for the primary full cohort LB pathology meta-analysis and x-axis shows the base-pair position. Points show probe coverage for the EPIC array and are colored by their direction of effect in association with LB-stage. The highlighted blue region shows the differentially methylated region (DMR) identified from comb-p analysis. Below track shows the annotated transcripts for the region. The black dashed horizontal line represents nominal significance ($p < 0.05$).

Next, we were interested in exploring whether *SNCA*, or indeed any other genes, contained statistically formally defined differentially methylated regions (DMRs), consisting of multiple adjacent DMPs by performing comb-p analysis on the summary statistics from our primary full cohort LB pathology meta-analysis. Although this analysis did not highlight the *SNCA* region as a formal DMR, we did identify three significant DMRs (**Supplementary Table 6**) overlapping the genes *LTF* (**Figure 3B**, Chr3:46506206-46506519, Šidák corrected p-value = 2.69×10^{-7}), the *NDRG4* (**Figure 3C**, Chr16:58535416-58535556, Šidák corrected p-value = 9.76×10^{-6}) and *MYO16* (**Figure 3D**, Chr 13:109741030-109741117, Šidák corrected p-value = 9.18×10^{-6}).

Exploring cortical LB associated methylation changes in the context of other neurodegenerative diseases

Next, we sought to investigate the disease specificity of the LB associated DMPs we had identified in our primary full cohort LB pathology meta-analysis by comparing these results to summary statistics in previously reported EWASs in AD and Huntington's disease (HD) brain samples. For AD associated effects, we utilized the summary statistics from a prior meta-analysis of NFT pathology in the cortex (Smith et al., 2021), performed on the Illumina Infinium Methylation 450K array and encompassing data from 1,408 individuals. For HD associated effects, we used a recently generated case-control cohort of 41 individuals and encompassing matched EPIC array data from the entorhinal cortex (n =38) and striatal (n = 37) brain regions (Wheildon et al., 2025). Taking the effect sizes for the Braak-LB associated DMPs from our primary full cohort LB pathology meta-analysis at a suggestive significance threshold ($p < 1 \times 10^{-5}$, n = 72 loci), we found a significant overlap with the direction of effect to Braak NFT associated changes for the 21 CpGs that overlapped between the studies (i.e. present across both array platforms) (**Figure 4A&B**, **Supplementary Table 7A**, binomial test probability = 0.81, q = 0.011), with 17 of the common 21 CpGs showing the same direction of effect. Similarly, we also observed a significant overlap in the direction of effect for the 72 Braak-LB associated DMPs with HD-associated changes at these CpG sites in the entorhinal cortex (**Figure 4A&C**, **Supplementary Table 7A**, binomial test probability = 0.74, $q = 2.3 \times 10^{-4}$), with 53 of the 72 CpGs assessed across both studies showing the same direction of effect. When we took the Bonferroni significant Braak NFT associated DMPs from the Smith et al study ($p < 1.24 \times 10^{-7}$, n = 208 loci present on the EPIC array), we found a significant overlap in the direction of effects to Braak-LB associated changes at these CpG sites (**Figure 4A&D**,

Supplementary Table 7B, binomial test probability = 0.89, q = 9.24 x 10^{-33}), with 186 of these 208 sites showing the same direction of effect. However, we did not observe a significant overlap in the direction of effect for these NFT-associated sites with HD-associated changes in the entorhinal cortex (**Supplementary Table 7B**). Notably, neither the Braak-LB DMPs, nor the Braak NFT DMPs showed any significant overlap in the direction of effect with the midbrain HD-associated effects in the striatum (**Supplementary Table 7A&B**), indicating effects are cortex specific. Together, this suggests a shared neurodegenerative methylation signal in the cortex across these three primary pathologies. However, although a shared cortical methylation signature is apparent across neurodegenerative diseases from our comparison of direction of effects, it is worth noting that the top-ranked loci are distinct across the different diseases. Indeed, for the 30 FDR significant LB-associated DMPs in our primary full cohort meta-analysis, only cg13847853 was Bonferroni-significant in the Braak NFT meta-analysis performed by Smith et al. (2021). Outside of this overlapping locus, no other sites even showed suggestive significance ($p < 1 \times 10^{-5}$) in either the Braak NFT or HD EWASs (**Supplementary Table 8**) and similarly, none of the Bonferroni DMPs from the Braak-NFT meta-analysis (aside from cg13847853) showed suggestive significance ($p < 1 \times 10^{-5}$) in the primary full cohort LB pathology meta-analysis, nor in the HD EWASs (**Supplementary Table 9**). This indicates that the most robust cortical DMPs in each neurodegenerative disease are specific to that disease.

Epigenetic prediction models of cortical pathology show best sensitivity and most balanced prediction for their specific pathological outcome.

Given that an epigenetic predictor has been previously generated for NFT pathology (Smith et al., 2021) and the high comparability we observed between LB and NFT pathology associated methylation profiles, we next sought to generate an epigenetic predictor for LB pathology and compare the ability of these epigenetic signatures to distinguish either pathology. Consistent with previous studies, we employed an elasticnet predictor model. For LB pathology prediction, models were trained on the UKBBN and NBB cohorts for binary cortical LB status (low pathology: Braak LB 0 vs high pathology: Braak LB 5-6) using the 48 methylated sites reaching the suggestive significance threshold ($p < 1 \times 10^{-5}$) in our secondary pure LB sensitivity meta-analysis. This was chosen as this analysis excluded the BDR cohort, which could then be used for independent validation of the two pathology signatures. Following training, the elasticnet model retained 40 sites for optimum prediction of LB pathology (**Supplementary Table 10**) and achieved a moderate accuracy in the training cohort (Area under Receiver operator curve (AUC) = 0.86, Mathews Correlation Coefficient (MCC) = 0.54, Balanced Accuracy = 0.75). We compared these predictions to a model trained for binary NFT prediction, outlined in Smith et al. (2021) based on methylation at 110 loci.

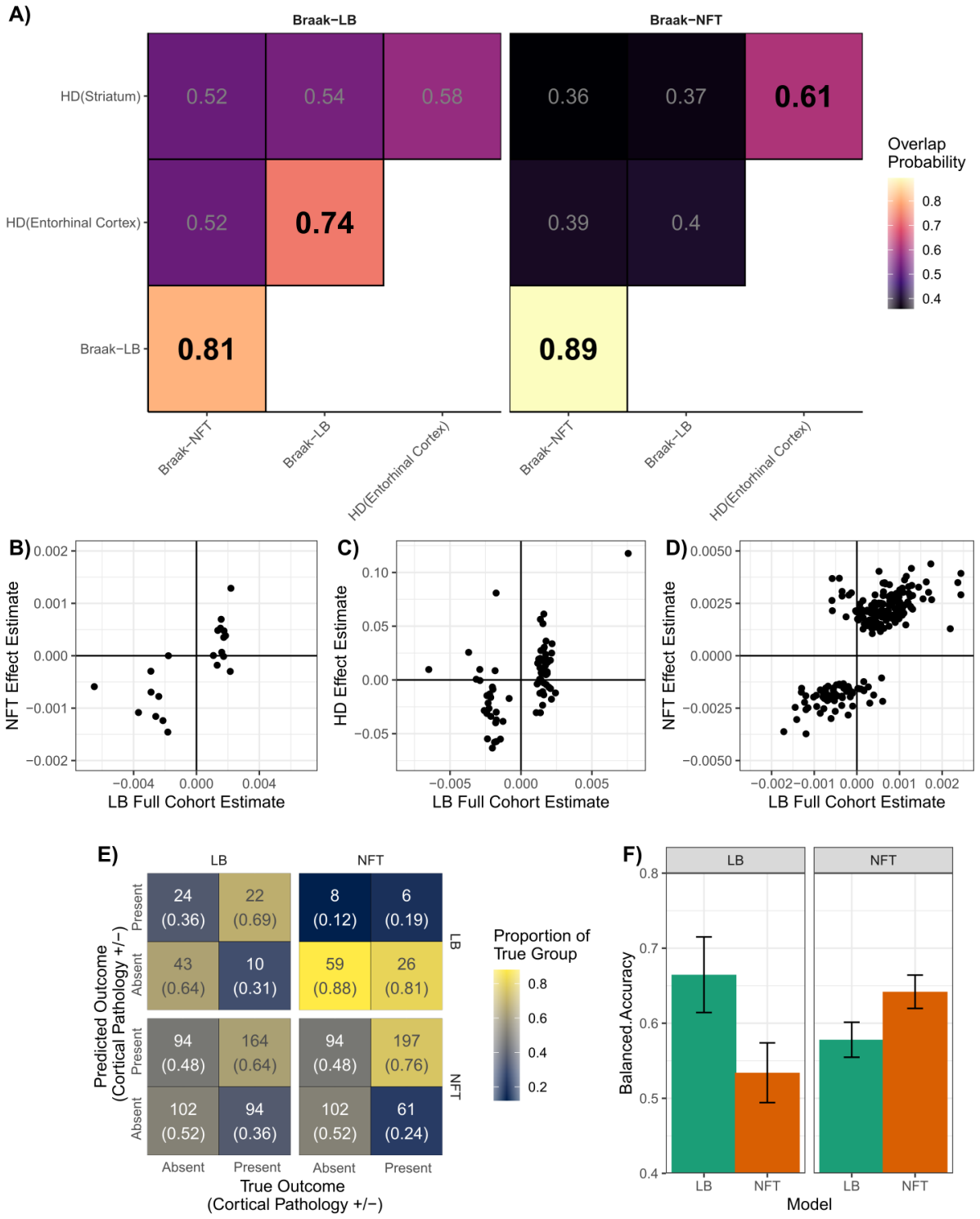

Figure 4. Summary of comparisons of epigenomic signatures between different pathologies and accuracy of specific epigenetic pathology predictors. **A)** Heatmap of overlap in direction of effect for the most significant LB-Braak associated sites ($p < 1 \times 10^{-5}$, left panel) and NFT-Braak associated sites ($p < 1.25 \times 10^{-7}$, right panel) with different neurodegenerative disease outcomes. Fill color is the overlap probability is direction of association between two overlapping summary statistics as calculated by the binomial sign test. Bolded tiles indicate an FDR significant test for significant overlap in directionality of associations. Braak NFT effects are taken from Smith et al. (2021) and Huntington's Disease effects from Wheildon et al. (2025). **B-D)** Scatterplots of DNA methylation associated with different pathologies**. B)** Shown for the top LB-associated loci is the comparison of effect size in cortex for LB and NFT (Smith et al., 2021) for the 21 overlapping sites across summary statistics, and **C)** for LB

and HD (Wheildon et al., 2025) for the 72 overlapping sites across summary statistics. **D**) shows the comparison of effect size in cortex for previously reported NFT associated loci (Smith et al., 2021) in our LB samples for the 208 sites overlapping across summary statistics. **E)** Contingency tables of multiple epigenetic based pathology prediction models for binary classification of cortical pathology. Pathological outcome used to train the model is displayed along the x-axis, with the pathological outcome tested along the y-axis. Tiles are colored by the proportion of the true group predicted and text shows number of cases (top) and proportion of true predicted (bottom). **F)** Bar-plots showing balanced accuracy for each prediction scenario. X-axis shows which model was employed; y-axis shows balanced accuracy of prediction (+/- Standard Error). True outcome tested shown above the top of each plot grid.

Both models were tested in the BDR cohort as this was not used for training (**Supplementary Table 11).** We tested the accuracy in predicting the cortical pathology used for training versus the other pathology. When assessing binary cortical LB status as the outcome, better prediction performance was observed for the model trained for LB cortical pathology (AUC = 0.68, MCC = 0.31, Balanced Accuracy = 0.66) than the model trained on NFT cortical pathology (AUC = 0.66, MCC = 0.09, Balanced Accuracy = 0.53) (**Figure 4E&F**, **Supplementary Table 12**). Notably, NFT trained prediction models lacked any sensitivity for discriminating cortical LB status. Similarly, when assessing binary cortical NFT status as the outcome, better prediction performance was observed for the model trained for NFT cortical pathology (AUC = 0.70, MCC = 0.29, Balanced accuracy = 0.64), than one trained for LB pathology (AUC = 0.61, MCC = 0.16, Balanced Accuracy = 0.58) (**Figure 4E&F**, **Supplementary Table 12**).

Methylation quantitative trait loci analysis prioritizes sites under genetic influence but does not support overlap with known genetic risk loci.

A number of studies have shown that DNA methylation can be influenced by genetic variation, commonly termed methylation quantitative trait loci (mQTLs). Given the size of our cohort, we utilized matched genotyping array data for 405 samples from the UKBBN cohort to test for mQTLs at the 30 FDR significant methylation sites nominated in our primary full cohort LB pathology meta-analysis. We identified 176 cis-mQTLs annotated to six methylation loci: cg05523624 (*GRM1*), cg09966204 (*MYO16*), cg07837822(*MYO16*), cg21912448 (*RERE*), cg15054019 and cg22516725 (*WWOX*) (**Supplementary Table 13, Supplementary Figure 4**), and four trans-mQTLs annotated to four methylation loci: cg05523624 (*GRM1*), cg10604836 (*PHACTR4*), cg06441533 (*GPX2*) and cg16262110 (*MTA1*) (**Supplementary Table 14, Supplementary Figure 5**). However, none of the SNPs corresponding to these mQTLs overlapped with GWAS hits reported in in summary statistics from GWAS of AD (Kunkle et al., 2019; Bellenguez et al., 2022), PD (Kim et al., 2024) or DLB (Chia et al., 2021).

***The SNCA* region shows enrichment of differentially methylated loci**

Finally, to test if genomic regions prioritized by GWAS of AD (Kunkle et al., 2019), PD (Kim et al., 2024) and DLB (Chia et al., 2021) show enrichment for LB pathology associated methylation, we employed Brown's method to combine p-values across the disease-

associated linkage disequilibrium (LD) regions (**Supplementary Table 15**). Across the three disease GWASs tested, only the *SNCA* region, as annotated in the recent DLB (Chr4: 90743331 – 91005096, q = 0.0099) and PD GWAS (Chr4: 89835093 – 91453046, q = 0.015) showed significance after multiple testing correction. This included the seven CpG sites that we prioritized after the RRA analysis.

DISCUSSION

In this study we present a meta-analysis of cortical DNA methylation associated with LB pathology. We find evidence of significant differential methylation at 30 loci across the genome, the top three of which: cg27481153 (*UBASH3B)*, cg08577553 (*PTAFR*) and cg13847853, reached the most stringent cutoff for genome-wide interpretation. We find evidence that the functional annotations enriched in prioritized loci are related to a number of brain relevant traits including neuronal and synaptic function, inflammation and vascular processes. Comparison of our results to previous EWASs of AD-related neuropathology (Braak NFT) and HD status indicates a shared epigenomic profile across some, but not all, neurodegenerative diseases. Notably we observe comparable cortical profiles of LB-pathology, HD-status and NFT-pathology, but minimal comparability between AD and HD profiles. Despite the evidence of shared epigenomic profiles however, we find that best balanced accuracy for cortical pathology prediction, using epigenomic profiles, was achieved using results determined for that specific pathology.

A number of the genes prioritized from the primary full cohort LB meta-analysis have been previously related to LB-related traits. *UBASH3B* encodes Ubiquitin Associated and SH3 Domain Containing B, which is highly expressed in brain tissue and has a variety of related functions in cell signalling (Vukojević et al., 2024). It has been previously associated in PD and DLB cortical contexts, reported as differentially expressed in single cell analyses of prefrontal cortex astrocytes (Zhu et al., 2024) and inhibitory neurons of the anterior cingulate cortex (Feleke et al., 2021). Rare variants in the gene have also been associated with serum total tau levels in an exome sequencing study (Sarnowski et al., 2022). *PTAFR* encodes Platelet Activating Factor Receptor, highly expressed in brain tissue and implicated in cell signalling via the NF-κB pathway. It has been reported to be differentially expressed in AD hippocampal tissue (Liu et al., 2022) and is implicated in mediating astrocytic inflammatory responses (Hans et al., 2024). cg13847853 is a more perplexing site in terms of functional annotation but has been previously associated with AD NFT related pathology (Smith et al., 2021). It resides between a long non-coding RNA (LINC00974) and the gene *KRT19*. *KRT19* is minimally expressed in brain, although it has been associated on a proteomic level in the

periphery to amyloid beta pathology (Duggan et al., 2024). Further work in required to elucidate the downstream regulatory impact of this methylation site.

Of the FDR significant differentially methylated loci, a number have been previously associated with parkinsonian and LB related traits. *WWOX*, encoding WW Domain Containing Oxidoreductase, is a gene which is linked to autosomal recessive neurodevelopmental disorders (Repudi et al., 2021), but has also been shown in large GWAS to be associated with both AD status (Kunkle et al., 2019) and development of cognitive decline in PD (Liu et al., 2021). Differential methylation of *PTPRN2*, encoding Protein Tyrosine Phosphatase Receptor Type N2 has been reported in sorted cell populations of parkinsonian cortical regions (Kochmanski et al., 2022), as well as in the substantia nigra (Young et al., 2019). It has been reported as differentially methylated in PD blood samples in association with worsening motor progression (Chuang et al., 2019).

To address the potential for confounding AD related NFT pathology, we utilized a second meta-analysis restricted solely to samples with minimal co-pathology as defined by Braak LB Staging. This reduced the total viable sample size by around 36%, from 1,239 samples to 798 samples and, perhaps unsurprisingly, resulted in far fewer sites passing multiple testing correction. Solely cg13847853, the topmost associated loci in our primary full cohort meta-analysis, retained genome-wide significance. Notably however, there was a striking concordance in estimated effects between the two meta-analysis, which we interpret as evidence that the LB-stage associated effects from our primary analysis are not contingent on the presence of co-incident NFT pathology.

A number of the post-hoc tests on our results implicate epigenetic changes in the *SNCA* gene, despite this region not passing the multiple testing threshold used in our primary or secondary meta-analyses. In a targeted assessment of the gene, we found evidence of hypomethylation in a number of sites in the 5'-region of the gene, which we believe warrants highlighting given that multiple other studies have reported the same phenomena in relation to LB disease (Ai et al., 2014; Jowaed et al., 2010; Matsumoto et al., 2010; Desplats et al., 2011; Kantor et al., 2018). Furthermore when employing a method to aggregate p-values from our meta-analysis results based on genetic regions reported from related GWAS, we found that the only significantly enriched region corresponded to the *SNCA* region reported in the most recent PD (Kim et al., 2024) and DLB (Chia et al., 2021) GWASs. Given that *SNCA* differential methylation has a reported cell-type specific effect (Gu et al., 2021), future studies looking at cell type specificity of DNA methylation may yield sites in the gene at genome-wide significance.

We further find evidence of a shared epigenomic signature across multiple neurodegenerative diseases and pathologies. There was a clear comparability between epigenetic effects for LB and NFT pathologies in the cortex, indicating a level of shared molecular processes related to both pathologies. However, notably only cg13847853 was associated at genome-wide significance in both analyses, indicating that despite a shared profile between the two, the prioritization of individual processes may differentiate the different pathologies. Indeed, this indication of a level of unique signature to either pathology is displayed in our exploration of epigenomic prediction models, where best balanced accuracy was achieved only when using a model trained for the specific pathology being predicted. This shared effect is consistent with other modalities of genetic and biological data, with genetic risk in genes such as *CLU*, *WWOX* and *GRN* (Wainberg et al., 2023), as well as the *HLA* region (Stolp Andersen et al., 2022) having been shown to have associated overlap between PD and AD and evidence of a level of shared transcriptomic alteration in the brain of DLB and AD patients (Olney et al., 2024). Perhaps more surprisingly was evidence found here between LB and HD associated epigenomic profiles, specific to the cortex. This shared effect did not appear to be indicative of a broad neurodegenerative signal, as no evidence of comparability was seen between HD and NFT pathological profiles. Similarly, we did not find evidence of shared profiles with HD associated changes in the striatum. Given that HD is caused by a highly penetrant autosomal dominant genetic defect and shares minimal pathology with LBD, this finding is perplexing. One potential explanation is that both diseases are marked by a shared degeneration of the striatal regions and the similar cortical epigenomic profiles may represent a secondary signature of midbrain neurodegeneration. Further work is needed to determine if this shared epigenomic profile we observed between these differing movement disorders represents a potential shared biological etiology or secondary effects to other common features of the two conditions.

We found evidence that some of the FDR significant methylation sites identified in our primary meta-analysis have evidence of genetic influence from our mQTL calling. However, we found no evidence that the genetic variants prioritized from this analysis are associated with neurodegeneration related phenotypes from previous GWAS. This is in-keeping with similar findings from previous meta-analyses of neurodegenerative pathologies which have failed to find evidence of pleiotropy between AD genetic risk variants and mQTLs associated with EWAS prioritised methylation sites (Smith et al., 2021).

One limitation of our study is the quantified neuropathological outcomes used to determine association and control for confounding covariance. In this analysis we have used Braak LB

Stage, due to its use in previous studies (Pihlstrøm et al., 2022) of this type both for LBD and AD. Although Braak LB Stage is a useful instrument in assessing PD-relevant pathology progression, its utility in the broad context of LBDs, in particular DLB, is highly questioned. Indeed alternate staging schemes focus more on categorically subtyping pathological LB by its distribution in different brain regions (Attems et al., 2021) as opposed to an ordinal semi-quantitative scheme that assumes pathology initiates in the brainstem. Thus, in our analysis, samples which are grouped into specific Braak Stages may represent highly variable LB pathology burden in the cortical regions we are assessing. This decision was chosen for practicality to allow for a harmonized measure between this study and previous EWASs. Braak LB Staging was also the most represented pathological staging scheme in the brain bank records that we had access to. Similarly, although we made efforts to stratify and control for AD co-pathology as measured by Braak NFT Stage, we did not apply any controlling measures for amyloid pathology. This is because measurements of amyloid deposition, such as the Thal stage, were absent for a large proportion of available cases and thus could not be adequately controlled for. One challenge when studying post-mortem brain tissue in neurodegenerative diseases is the impact of neuronal cell loss, and gliosis on cell populations, which may impact the DNA methylation signatures observed in disease. Although we have attempted to mitigate this by controlling for the proportions of different neuronal and glial cell types, future analyses should be undertaken on sorted cell populations in order to identify cell-type specific signatures. Differences in the cell type deconvolution model used in this study, which resolves five cellular proportions, compared to less-granular models employed in previous, for example the Braak NFT meta-analysis (Smith et al., 2021), which resolved two, may also account for differences in study results with previous EWASs in LBDs. Moreover, recently developed soma isolation methods have shown utility in assessing neurons specifically bearing NFT pathology in AD cortex and could be applied to the study of LBs in LBDs (Otero-Garcia et al., 2022).

In summary, we have undertaken the largest meta-analysis of DNA methylation in LBDs to date, highlighting robust methylation alterations at 30 loci, and highlighting epigenetic alterations in *SNCA* in disease. Future studies warrant DNA methylomic analyses of well-characterized cohorts with detailed ante-mortem and post-mortem clinical and pathological assessments, in order to identify signatures that distinguish between different LBDs that show similar pathological profiles with more distinct clinical symptoms. The integration of DNA methylation data with other epigenetic marks and transcriptional profiling will allow the identification of disease signatures that impact at multiple layers of genomic regulation and may represent novel candidates when developing pharmacological intervention strategies.

METHODS

Cohort Descriptions

Samples were sourced from the UK Brain Bank Network (UKBBN), an online database covering brain bank centers across the UK and annotated with demographics, neuropathological and clinical assessments. All available records on the UKBBN were downloaded (June 2019) for manual selection. First, to determine LB positive case availability, records were filtered on a basis of neuropathological diagnostic criteria. Only cases with an annotation of Braak LB Stage of 3-6, or annotation of neocortical or limbic LB pathology were selected as LBD cases. The majority of samples matching our search criteria were found in brain banks at Oxford, Newcastle, Imperial College London and University College London. Samples were sourced on the basis of a primary diagnosis of either PD or DLB, either in available clinical records or at post-mortem examination. Samples were included if they had a primary neuropathologically confirmed diagnosis of PD or DLB and, where primary diagnosis was absent, had a “High” assessment of the likelihood that the pathological profiles were associated with typical DLB clinical syndrome from the 2017 Lancet criteria (McKeith et al., 2017). Exclusions were made for non-sporadic synucleinopathies or misdiagnosed primary symptoms (e.g., multiple system atrophy (MSA), PSP etc.), severe cerebrovascular disease or TDP-43 pathology, as well as removing cases annotated with amygdala predominant LB pathology. Seventy-one cases had annotation for LBD relevant pathology following the 2009 Unified staging scheme but lacked Braak LB staging annotation (Beach et al., 2009). To harmonize these annotations for analysis alongside the Braak scheme, records were converted in accordance with the BrainNet Europe Consortium (Alafuzoff et al., 2009). Sixty-one cases with “Neocortical Lewy Body Disease” were annotated as Braak LB Stage 6. The remaining ten cases showed evidence from the available additional neuropathology notes of LB pathology in the temporal cortex or cingulate gyrus and were annotated as Braak LB Stage 5. From this criterion we selected 28 cases with Braak LB Stage 3, 38 cases with Braak LB Stage 4, 39 cases with Braak LB Stage 5 and 211 cases with Braak LB Stage 6. An additional 101 control individuals without neurological disease were sourced, which were chosen to exclude significant cerebrovascular pathology or substantial AD-related pathology (Braak NFT stage > 2). In total, a set of 417 total donors were chosen for our study, with two brain regions sourced for the majority of individuals. These brain regions were the ACC (Brodmann Area 24) and the PFC (Brodmann Area 9). All samples received for our study had informed consent at local brain banks, covered under individual ethical agreements at the center (REC references 24/NE/0012, 15/SC/0639, 18/LO/0721, 23/WA/0273). Ethical approval for our study was granted from the University of Exeter Medical School Research Ethics Committee (13/02/009).

Data for the Netherlands Brain Bank (NBB) cohort has been previously detailed in Pihlstrøm et al., 2022, where they had analysed PFC tissue from 73 control, 29 incidental Lewy Body disease, 139 PD (of which 74 were PDD), and 81 DLB patients (Pihlstrøm et al., 2022). Data from the Brains for Dementia Research Cohort (BDR) was previously detailed in Shireby et al., 2022 (Shireby et al., 2022). Neurological controls were selected with absence of LB-pathology and low AD co-pathology (Braak NFT < 3), along with the absence of significant neuropathological co-pathology (TDP-43 pathology, gross infarction, severe cerebrovascular disease). Eight samples overlapped between the UKBBN and BDR cohort and were removed from the BDR cohort prior to analysis. Case samples were selected in keeping with the same criteria as the UKBBN. A final set of 116 samples from the BDR cohort were used for the meta-analysis.

Sample Preparation and Methylomic Profiling

For the UKBBN cohort, tissue pieces ranging between 25-35 mg were cut from frozen PFC or ACC tissue before being milled over liquid nitrogen. Following tissue grinding DNA was extracted using the Qiagen AllPrep DNA/RNA/miRNA Universal kit according to the manufacturer's instructions and stored at 4°C. 500ng of DNA from each sample was bisulfite treated using the Zymo EZ-96 DNA methylation Gold kit. Methylomic profiling was completed after sample randomization using the Illumina Infinium MethylationEPIC v1.0 BeadChip.

DNA Methylation Analysis, Quality Control and Normalization

Data processing was performed using R, and signal intensity files were loaded into R using the minfi package (Aryee et al., 2014). All data was subjected to a thorough quality control (QC) pipeline using the minfi (Aryee et al., 2014) and wateRmelon packages (Pidsley et al., 2013). A *MethylumiSet* object was created from iDATs using the *readEPIC* function from wateRmelon (Pidsley et al., 2013) and an *RGChannelSet* was created using the minfi package (Aryee et al., 2014). Samples were excluded from further analysis for the following reasons: (1) they had a median methylated or unmethylated sample intensity < 1500 or < 1000, respectively, (2) that the bisulfite conversion efficiency was < 80%, (3) there was a mis-match between reported and predicted sex, (4) if the sample was determined to be an outlier using the *outlyx* function or, (5) if the samples were found to be cryptically related to one another or unrelated to its matched sample from the other brain region. Finally, using the *pfilter* function in the WateRmelon package (Pidsley et al., 2013) samples with a detection p-value > 0.05 in > 5% of probes, probes with < three beadcount in 5% of samples and probes having 1% of samples with a detection p-value > 0.05 were also removed. Following QC, samples not passing the aforementioned checks were removed and quantile normalization was performed using the *dasen* function in the wateRmelon package (Pidsley et al., 2013). Beta values were

extracted for further analysis. Cell type proportion calculations were implemented using the projectCellTypeWithError() function within the CETYGO package (Vellame et al., 2023), using the reference panel resolving enriched profiles for GABAergic neuron, Glutamatergic neuron, Oligodendrocyte, Microglia and Astrocyte reference data (Hannon et al., 2024).

Within cohort epigenome wide association assessment

Prior to meta-analysis, the association with LB Braak stage was assessed within each cohort in a harmonized approach. Within each cohort, linear models were fit using the base lm() function in R to test for associations between LB Braak Stage and DNA methylation at each site of the genome. This is displayed by the following equation for the NBB and BDR analyses:

$$CpG\ Site \sim Braak\ LB\ Stage + Age + Sex + PMI + Cell\ Proportion + Batch + Braak\ NFT\ Stage \ldots$$

For the UKBBN analysis, given two brain regions were present per individuals, this caused a violation of linear regression by non-independence between samples type. To correct for this, a mixed effect model was employed using the lme() function within the nlme package. Brain region was included as a fixed effect covariate and individual ID was supplied as a random-intercept covariate to account for paired observations. This can be displayed in the following formula:

$$CpG\ Site \sim Braak\ LB\ Stage + Age + Sex + PMI + Cell\ Proportion + Batch + Braak\ NFT\ Stage + (1|Individual) \ldots$$

Consistent covariates of age, sex, PMI, cell proportions and Braak NFT stage were included in all three cohorts. For the UKBBN and BDR cohorts, brain bank source and array plate batch were included as processing batch variables. For a small subset of the UKBBN donors, PMI values were missing (n = 12) and in these cases, mean imputation was used to fill missing values. This method was justified based on previous data exploration for best methods to deal with missingness in phenotypic data (Harvey 2022). For NBB, only processing plate batch was included. For each cohort, model p-value inflation was assessed genome wide and surrogate variables added to reduce the lambda value below a 1.2 threshold. One surrogate variable was included for BDR and three were included for NBB, with no surrogate variables required to reduce inflation in UKBBN (**Supplementary Figure 1**).

Meta-analysis

Estimated regression coefficients and standard errors were extracted from each model and used for meta-analysis of all probes overlapping each dataset (n = 774,310). Harmonized models were meta-analysed using the metagen function in the meta R package (Balduzzi et al., 2019), as had been employed for previous EWAS meta-analyses (Pihlstrøm et al., 2022; Shireby et al., 2022; Fodder et al., 2023; Smith et al., 2021), which applies an inverse variance weighting. Both fixed and random effects were assessed, with the fixed effects model being the primary interpreted results. In addition to fixed and random effects modelling statistics (Effect estimates, standard error and p-values), the I^2 heterogeneity measure and p-values were also extracted.

For interpretation of results, a strict genome-wide significance threshold was based on a previous simulation and permutation testing study to define a significance level as determined by Mansell and colleagues (Mansell et al., 2019). This approach sets a consistent significance threshold of p-value < 9×10^{-8} for any study utilizing the Illumina EPIC array and was determined based on multiple permutations of null EWAS study scenarios to determine a 5% family wise error rate. A less stringent multiple testing False Discovery Rate (FDR) significance threshold (corrected p-value (q-value) < 0.05) was also used in our study. Finally for more exploratory post-hoc analysis, a more lenient suggestive threshold was applied of uncorrected p-value < 1×10^{-5}.

Differentially methylated region analysis

To identify differentially methylated regions (DMRs) from summary statistics from our meta-analyses, we employed the combined p-values method as implemented in the python package comb-p (Pedersen et al., 2012), which identifies DMRs based on a defined sliding window, correcting for spatial autocorrelation between adjacent methylation sites. We performed this with the default settings for consistency with prior meta-analyses, with a distance of 500 base-pairs (bp) and a seeded p-value of 1×10^{-4}. Significant DMRs were defined as those with a Sidak's multiple testing correction p-value < 0.05 and with ≥ two methylation sites residing in the identified DMR. For plotting, EnsDb.Hsapiens.v75 and GenomicRanges were used to extract annotated transcripts for genome build 37 hg19.

Gene ontology analysis

Gene ontology (GO) analysis was performed using the package methylGSA function methylRRA (Ren and Kuan, 2018). This method assesses genome wide summary statistics as summarized by p-values and aggregates them around gene annotations, controlling for the number of CpGs annotated to differing genes. We utilised the overrepresentation analysis approach, which applies a within gene Bonferroni correction and a across gene FDR

correction to prioritize genes for ontological enrichment analyses. Given the overlap of similar ontology terms, for interpretation of significant enriched terms in our results, we further employed the REVIGO method, as implemented in the rrvgo R package (Sayols, 2023) using default parameters to identify shared parent terms for closely related GO annotations.

Cross disease epigenomic signature comparison

Assessment of overlap between EWASs was conducted by assessing the directionality of estimated effects in available summary statistics. To statistically compare shared direction of effects, a one-sided binomial sign test was performed to test for greater than expected overlap in association directionality. For comparison to AD related Braak NFT associated signatures, summary statistics were sourced from Smith et al. 2021, which had performed a cross-cortical meta-analysis (Smith et al., 2021). This had utilized 1,408 unique donors, which had been profiled on the Illumina Infinium Methylation 450K BeadChip. For assessment of HD-associated signatures, summary statistics were sourced from Wheildon et al. (2025). This included matched data for 38 entorhinal cortex and 37 striatal samples, profiled on the Illumina EPIC array. Our Braak NFT EWAS signature comprised the 208 sites on the EPIC array corresponding to the 220 sites passing Bonferroni significance in Smith et al. (2021). For the Braak LB signature, given that more modest p-values were identified, we used the 72 sites passing our suggestive p-value threshold of 1×10^{-5} in the primary full cohort LB pathology meta-analysis. Following all comparisons tested, FDR correction was applied for interpreting the significant overlap in shared direction of association.

Epigenetic classification analysis

To further compare the epigenetic signatures of the Braak LB and Braak NFT meta-analysis, we used an elasticnet model trained using loci prioritised from the EWAS. The LB model was trained in the UKBBN and NBB pure pathology subset, using the 48 loci passing suggestive association ($p < 1 \times 10^{-5}$) in the secondary pure LB pathology subset cohort meta-analysis. The BDR dataset was used for validation to account for data leakage and non-independence between training and testing cohorts. Models were trained for binarized prediction of cortical LB pathology (total n = 625, Braak LB 0: n = 246, Braak LB 5-6: n = 379) across 10-fold cross validated folds and with the alpha value set to 0.5 (**Supplementary Table 8 & 9**). This model was then tested in the BDR cohort using the same samples employed for the primary meta-analysis, binarized for cortical pathology (total n = 99, Braak LB 0: n = 67, Braak LB 5-6: n = 32). To compare to predictions for Braak NFT pathology, a similar model based on 110 loci from Smith et al., (2021), previously detailed in their publication was tested on the same subset. To assess the accuracy of binarized cortical NFT prediction, the same subset of AD relevant cases and controls was used as those tested in the original publication (total n = 454,

Braak NFT 0-II: n = 196, Braak NFT V-VI: n = 258). Models were assessed for accuracy using Area Under the receiver operator curve (AUC), Matthews Correlation Coefficient (MCC) and balanced accuracy.

Methylation Quantitative Loci Analysis and Genomic Enrichment Analysis

Methylation quantitative loci (mQTLs) were identified in the UKBBN data using a set of 473 samples with matched Illumina Global Screening Array (GSA) genotyping data. mQTLs were tested solely for the 30 loci at FDR significance in the primary full cohort LB pathology meta-analysis. The R package matrix eQTL was used to identify methylation sites with significant association to genetic loci (Shabalin, 2012). Methylation beta-values were tested against genotype (coded additively) utilizing a linear model for association testing while adjusting for confounders of age and sex.

Matrix eQTL was run in linear model mode with an additive genetic model to assess *cis*- and *trans*-mQTLs. *Cis*-mQTLs were defined as SNPs located within ±1 Mb of the associated CpG site, while *trans*-mQTLs correspond to SNPs > 1 Mb from the CpG. The significance threshold was adjusted for multiple testing using FDR correction, with a significance threshold of $q < 0.05$.

To test for genomic enrichment in LB associated methylation loci in known regions prioritized by prior GWAS, we employed Brown's method, as implemented in the EmpiricalBrownsMethod R package to aggregate p-values across multiple methylation loci (Poole, 2024). Regions in linkage disequilibrium (LD) with primary loci in GWAS were extracted for AD, PD and DLB. For PD (Kim et al 2024) and AD (Kunkle et al 2019), reported regions were taken directly from the supplementary material of the respective study. For DLB (Chia et al. 2021), as regions were not directly reported, regions were manually annotated based on the minimum and maximum position of variants at genome wide significance ($p < 5 \times 10^{-8}$) in the genome-wide summary statistics around the five primary loci reported in the study. P-values were FDR corrected to account for the number of total genomic regions tested. Methylation beta matrixes were z-score normalized using the scale() function in R within each cohort, to allow for the correlation calculations within the Brown's methodology accounting for inter-cohort variability whilst retaining the inter-site correlations.

DATA AVAILABILITY

Methylation data, genotyping data and available phenotypic data used in primary analyses for the UKBBN cohort will be made available on the Gene Expression Omnibus (GEO) Platform upon final publication. Data for the NBB cohort is available via GEO at accession number

GSE203332. Data for the BDR cohort is available via GEO at accession number GSE197305 and additional donor data is available via Dementia Platform UK (https://portal.dementiasplatform.uk/).

Genome-wide summary statistics for meta-analyses performed in this study are available at https://github.com/UoE-Dementia-Genomics/LB-Meta-Analysis

CODE AVAILABILITY

Analysis scripts used in this manuscript are available at https://github.com/UoE-Dementia-Genomics/LB-Meta-Analysis

References

Ai S-x, Xu Q, Hu Y-c, et al. (2014) Hypomethylation of SNCA in blood of patients with sporadic Parkinson's disease. *Journal of the Neurological Sciences* 337(1): 123-128.

Alafuzoff I, Ince PG, Arzberger T, et al. (2009) Staging/typing of Lewy body related α-synuclein pathology: a study of the BrainNet Europe Consortium. *Acta Neuropathologica* 117(6): 635-652.

An D and Xu Y (2024) Environmental risk factors provoke new thinking for prevention and treatment of dementia with Lewy bodies. *Heliyon* 10(9): e30175.

Aryee MJ, Jaffe AE, Corrada-Bravo H, et al. (2014) Minfi: a flexible and comprehensive Bioconductor package for the analysis of Infinium DNA methylation microarrays. *Bioinformatics* 30(10): 1363-1369.

Attems J, Toledo JB, Walker L, et al. (2021) Neuropathological consensus criteria for the evaluation of Lewy pathology in post-mortem brains: a multi-centre study. *Acta Neuropathologica* 141(2): 159-172.

Balduzzi S, Rücker G and Schwarzer G (2019) How to perform a meta-analysis with R: a practical tutorial. *Evid Based Ment Health* 22(4): 153-160.

Beach TG, Adler CH, Lue L, et al. (2009) Unified staging system for Lewy body disorders: correlation with nigrostriatal degeneration, cognitive impairment and motor dysfunction. *Acta Neuropathol* 117(6): 613-634.

Bellenguez C, Küçükali F, Jansen IE, et al. (2022) New insights into the genetic etiology of Alzheimer's disease and related dementias. *Nature Genetics* 54(4): 412-436.

Ben-Shlomo Y, Darweesh S, Llibre-Guerra J, et al. (2024) The epidemiology of Parkinson's disease. *The Lancet* 403(10423): 283-292.

Chia R, Sabir MS, Bandres-Ciga S, et al. (2021) Genome sequencing analysis identifies new loci associated with Lewy body dementia and provides insights into its genetic architecture. *Nat Genet* 53(3): 294-303.

Chuang YH, Lu AT, Paul KC, et al. (2019) Longitudinal Epigenome-Wide Methylation Study of Cognitive Decline and Motor Progression in Parkinson's Disease. *J Parkinsons Dis* 9(2): 389-400.

De Jager PL, Srivastava G, Lunnon K, et al. (2014) Alzheimer's disease: early alterations in brain DNA methylation at ANK1, BIN1, RHBDF2 and other loci. *Nat Neurosci* 17(9): 1156-1163.

Desplats P, Spencer B, Coffee E, et al. (2011) Alpha-synuclein sequesters Dnmt1 from the nucleus: a novel mechanism for epigenetic alterations in Lewy body diseases. *J Biol Chem* 286(11): 9031-9037.

Duggan MR, Gomez GT, Joynes CM, et al. (2024) Proteome-wide analysis identifies plasma immune regulators of amyloid-beta progression. *Brain Behav Immun* 120: 604-619.

Feleke R, Reynolds RH, Smith AM, et al. (2021) Cross-platform transcriptional profiling identifies common and distinct molecular pathologies in Lewy body diseases. *Acta Neuropathol* 142(3): 449-474.

Fodder K, Murthy M, Rizzu P, et al. (2023) Brain DNA methylomic analysis of frontotemporal lobar degeneration reveals OTUD4 in shared dysregulated signatures across pathological subtypes. *Acta Neuropathol* 146(1): 77-95.

Gu J, Barrera J, Yun Y, et al. (2021) Cell-Type Specific Changes in DNA Methylation of SNCA Intron 1 in Synucleinopathy Brains. *Front Neurosci* 15: 652226.

Hannon E, Dempster EL, Davies JP, et al. (2024) Quantifying the proportion of different cell types in the human cortex using DNA methylation profiles. *BMC Biology* 22(1): 17.

Hans S, Stanton JE, Sauer AK, et al. (2024) Polar lipids modify Alzheimer's Disease pathology by reducing astrocyte pro-inflammatory signaling through platelet-activating factor receptor (PTAFR) modulation. *Lipids in Health and Disease* 23(1): 113.

Jowaed A, Schmitt I, Kaut O, et al. (2010) Methylation regulates alpha-synuclein expression and is decreased in Parkinson's disease patients' brains. *J Neurosci* 30(18): 6355-6359.

Kantor B, Tagliafierro L, Gu J, et al. (2018) Downregulation of SNCA Expression by Targeted Editing of DNA Methylation: A Potential Strategy for Precision Therapy in PD. *Molecular Therapy* 26(11): 2638-2649.

Kim JJ, Vitale D, Otani DV, et al. (2024) Multi-ancestry genome-wide association meta-analysis of Parkinson's disease. *Nature Genetics* 56(1): 27-36.

Kochmanski, J., Kuhn, N. C., & Bernstein, A. I. (2022). Parkinson's disease-associated, sex-specific changes in DNA methylation at PARK7 (DJ-1), SLC17A6 (VGLUT2), PTPRN2 (IA-2β), and NR4A2 (NURR1) in cortical neurons. *Npj Parkinson's Disease 2022 8:1*, *8*(1), 1–13. https://doi.org/10.1038/s41531-022-00355-2

Kunkle BW, Grenier-Boley B, Sims R, et al. (2019) Genetic meta-analysis of diagnosed Alzheimer's disease identifies new risk loci and implicates Aβ, tau, immunity and lipid processing. *Nature Genetics* 51(3): 414-430.

Lee DR, McKeith I, Mosimann U, et al. (2013) Examining carer stress in dementia: the role of subtype diagnosis and neuropsychiatric symptoms. *Int J Geriatr Psychiatry* 28(2): 135-141.

Liu G, Peng J, Liao Z, et al. (2021) Genome-wide survival study identifies a novel synaptic locus and polygenic score for cognitive progression in Parkinson's disease. *Nat Genet* 53(6): 787-793.

Liu J, Jiao L, Zhong X, et al. (2022) Platelet Activating Factor Receptor Exaggerates Microglia-Mediated Microenvironment by IL10-STAT3 Signaling: A Novel Potential Biomarker and Target for Diagnosis and Treatment of Alzheimer's Disease. *Front Aging Neurosci* 14: 856628.

Lunnon K, Smith R, Hannon E, et al. (2014) Methylomic profiling implicates cortical deregulation of ANK1 in Alzheimer's disease. *Nat Neurosci* 17(9): 1164-1170.

Mansell G, Gorrie-Stone TJ, Bao Y, et al. (2019) Guidance for DNA methylation studies: statistical insights from the Illumina EPIC array. *BMC Genomics* 20(1): 366.

Matsumoto L, Takuma H, Tamaoka A, et al. (2010) CpG demethylation enhances alpha-synuclein expression and affects the pathogenesis of Parkinson's disease. *PLoS One* 5(11): e15522.

McKeith IG, Boeve BF, Dickson DW, et al. (2017) Diagnosis and management of dementia with Lewy bodies: Fourth consensus report of the DLB Consortium. *Neurology* 89(1): 88-100.

Nalls MA, Blauwendraat C, Vallerga CL, et al. (2019) Identification of novel risk loci, causal insights, and heritable risk for Parkinson's disease: a meta-analysis of genome-wide association studies. *Lancet Neurol* 18(12): 1091-1102.

Olney KC, Rabichow BE, Wojtas AM, et al. (2024) Distinct transcriptional alterations distinguish Lewy body disease from Alzheimer's disease. *Brain* 148(1): 69-88.

Otero-Garcia M, Mahajani SU, Wakhloo D, et al. (2022) Molecular signatures underlying neurofibrillary tangle susceptibility in Alzheimer's disease. *Neuron* 110(18): 2929-2948.e2928.

Pedersen BS, Schwartz DA, Yang IV, et al. (2012) Comb-p: software for combining, analyzing, grouping and correcting spatially correlated P-values. *Bioinformatics* 28(22): 2986-2988.

Pidsley R, Y Wong CC, Volta M, et al. (2013) A data-driven approach to preprocessing Illumina 450K methylation array data. *BMC Genomics* 14(1): 293.

Pihlstrøm L, Shireby G, Geut H, et al. (2022) Epigenome-wide association study of human frontal cortex identifies differential methylation in Lewy body pathology. *Nat Commun* 13(1): 4932.

Poole W (2024) EmpiricalBrownsMethod: Uses Brown's method to combine p-values from dependent tests. *R package version 1.34.0*.

Ren X and Kuan PF (2018) methylGSA: a Bioconductor package and Shiny app for DNA methylation data length bias adjustment in gene set testing. *Bioinformatics* 35(11): 1958-1959.

Repudi S, Steinberg DJ, Elazar N, et al. (2021) Neuronal deletion of Wwox, associated with WOREE syndrome, causes epilepsy and myelin defects. *Brain* 144(10): 3061-3077.

Ricci M, Guidoni SV, Sepe-Monti M, et al. (2009) Clinical findings, functional abilities and caregiver distress in the early stage of dementia with Lewy bodies (DLB) and Alzheimer's disease (AD). *Arch Gerontol Geriatr* 49(2): e101-e104.

Robinson JL, Lee EB, Xie SX, et al. (2018) Neurodegenerative disease concomitant proteinopathies are prevalent, age-related and APOE4-associated. *Brain* 141(7): 2181-2193.

Sarnowski C, Ghanbari M, Bis JC, et al. (2022) Meta-analysis of genome-wide association studies identifies ancestry-specific associations underlying circulating total tau levels. *Communications Biology* 5(1): 336.

Sayols S (2023) rrvgo: a Bioconductor package for interpreting lists of Gene Ontology terms. *MicroPubl Biol* 2023.

Shabalin AA (2012) Matrix eQTL: ultra fast eQTL analysis via large matrix operations. *Bioinformatics* 28(10): 1353-1358.

Shireby G, Dempster EL, Policicchio S, et al. (2022) DNA methylation signatures of Alzheimer's disease neuropathology in the cortex are primarily driven by variation in non-neuronal cell-types. *Nat Commun* 13(1): 5620.

Smith AR, Smith RG, Pishva E, et al. (2019) Parallel profiling of DNA methylation and hydroxymethylation highlights neuropathology-associated epigenetic variation in Alzheimer's disease. *Clin Epigenetics* 11(1): 52.

Smith RG, Pishva E, Shireby G, et al. (2021) A meta-analysis of epigenome-wide association studies in Alzheimer’s disease highlights novel differentially methylated loci across cortex. *Nature Communications* 12(1).

Stolp Andersen, M., Tan, M., Holtman, I. R., Hardy, J., & Pihlstrøm, L. (2022). Dissecting the limited genetic overlap of Parkinson’s and Alzheimer’s disease. *Annals of Clinical and Translational Neurology*, *9*(8), 1289. https://doi.org/10.1002/ACN3.51606

Svendsboe E, Terum T, Testad I, et al. (2016) Caregiver burden in family carers of people with dementia with Lewy bodies and Alzheimer's disease. *Int J Geriatr Psychiatry* 31(9): 1075-1083.

Tsalenchuk M, Gentleman SM and Marzi SJ (2023) Linking environmental risk factors with epigenetic mechanisms in Parkinson’s disease. *npj Parkinson's Disease* 9(1): 123.

Vellame DS, Shireby G, MacCalman A, et al. (2023) Uncertainty quantification of reference-based cellular deconvolution algorithms. *Epigenetics* 18(1): 2137659.

Vukojević K, Šoljić V, Martinović V, et al. (2024) The Ubiquitin-Associated and SH3 Domain-Containing Proteins (UBASH3) Family in Mammalian Development and Immune Response. *Int J Mol Sci* 25(3).

Wainberg M, Andrews SJ and Tripathy SJ (2023) Shared genetic risk loci between Alzheimer’s disease and related dementias, Parkinson’s disease, and amyotrophic lateral sclerosis. *Alzheimer's Research & Therapy* 15(1): 113.

Young JI, Sivasankaran SK, Wang L, et al. (2019) Genome-wide brain DNA methylation analysis suggests epigenetic reprogramming in Parkinson disease. *Neurology Genetics* 5(4): e342.

Zhu B, Park J-M, Coffey SR, et al. (2024) Single-cell transcriptomic and proteomic analysis of Parkinson's disease brains. *Science Translational Medicine* 16(771): eabo1997.

ACKNOWLEDGEMENTS

We acknowledge the brain banks used in the sourcing of tissue, clinical and neuropathological data used in this study. These include the Oxford, UCL Queen's Square, Imperial College London Parkinson's disease Brain Bank and Newcastle Brain Banks.

FUNDING

This work was funded by research grants from the Medical Research Council (MRC (MR/S011625/1), the National Institute of Aging (NIA) of the National Institutes of Health (NIH) (R01AG067015), the Alzheimer's Society (AS-PG-16b-012), Alzheimer's Research UK (ARUK-PG2023A-037) and the Charles Wolfson Charitable Trust to KL, research grants from the Michael J Fox Foundation (MJFF-023152) and ZonMw Memorabel/Alzheimer Nederland Grant (733050516) to EP and a research fellowship from the Alzheimer's Society (AS-PDF-23-017) to JI.

Tissue for this study was provided by the Newcastle Brain Tissue Resource which is funded in part by a grant from the UK MRC (G0400074), by NIHR Newcastle Biomedical Research Centre and Unit awarded to the Newcastle upon Tyne NHS Foundation Trust and Newcastle University, and as part of the BDR Programme jointly funded by Alzheimer's Research UK and the Alzheimer's Society. The Parkinson's disease Brain Bank, at Imperial College London is funded by Parkinson's UK, a charity registered in England and Wales (258197) and in Scotland (SC037554). The Oxford Brain Bank, supported by MRC, the NIHR Oxford Biomedical Research Centre and the BDR programme, jointly funded by Alzheimer's Research UK and the Alzheimer's Society.

COMPETING INTERESTS

The authors declare no competing interests.

AUTHOR INFORMATION

JH, JI and ARS conducted laboratory experiments generating the DNA methylation data. JH undertook data analysis and bioinformatics, with support from MK, BC, RGS and GW. ZJ, EDP-F, TW, DL, DG, HB, JA and AT supported with sample characterization and selection.

GS, ED, LP and JM provided data for the meta-analysis. LC, CB, JO'B, DA and KL conceived the project. EP and KL supervised the project. JH, JI, EP and KL drafted the manuscript. All authors read and approved the final submission.

ETHICS DECLARATIONS

The authors declare no competing interests